



Influence of dislocation density on photoluminescence intensity of GaN

J.F. Fälth^{a,*}, M.N. Gurusinge^a, X.Y. Liu^a, T.G. Andersson^a, I.G. Ivanov^b,
B. Monemar^b, H.H. Yao^c, S.C. Wang^c

^aDepartment of Microtechnology and Nanoscience, Applied Semiconductor Physics-MBE, Chalmers University of Technology and Göteborg University, Göteborg S-412 96, Sweden

^bDepartment of Physics and Measurement Technology, Linköping University, S-581 83 Linköping, Sweden

^cInstitute of Electro-optical Engineering, National Chiao Tung University, 1001 Ta Hsueh Road, Hsinchu 300, Taiwan

Available online 11 February 2005

Abstract

The influence of dislocation density on photoluminescence intensity is investigated experimentally and compared to a model. GaN samples were grown by molecular beam epitaxy and metal-organic chemical vapour deposition. Different growth parameters and thicknesses of the layers resulted in different dislocation densities. The threading dislocation density, measured by atomic force microscopy, scanning electron microscopy and X-ray diffraction, covered a range from 5×10^8 to $3 \times 10^{10} \text{ cm}^{-2}$. Carrier concentration was measured by capacitance–voltage-, and Hall effect measurements and photoluminescence at 2K was recorded. A model which accounts for the photoluminescence intensity as a function of dislocation density and carrier concentration in GaN is developed. The model shows good agreement with experimental results for typical GaN dislocation densities, 5×10^8 – $1 \times 10^{10} \text{ cm}^{-2}$, and carrier concentrations 4×10^{16} – $1 \times 10^{18} \text{ cm}^{-3}$.

© 2005 Elsevier B.V. All rights reserved.

PACS: 81.15.Hi; 78.20.Bh; 61.72.Hh

Keywords: A3. Molecular beam epitaxy; B1. Nitrides; A1. Defects; A1. Photoluminescence; A1. Capacitance–voltage measurement; A1. Atomic force microscopy

1. Introduction

The components of the group III nitride system and their alloys are attractive materials for use in optoelectronic and high-temperature, high-power electronic applications. The wide bandgap and the excellent thermal- and chemical stability make

*Corresponding author. Tel.: +46 31 7723226;
fax: +46 31 7723085.

E-mail address: fredrik.falth@mc2.chalmers.se (J.F. Fälth).

them ideal candidates for devices. Existing nitride devices include visible- and ultraviolet (UV) light emitters, blue lasers and UV detectors. Most nitride device material is epitaxially grown. The main epitaxial techniques are metal-organic vapour phase epitaxy (MOCVD), plasma-assisted molecular beam epitaxy (MBE), or direct growth by MBE in ammonia. Lacking an affordable, high-quality lattice-matched substrate, growth of GaN is usually done on α -phase Al_2O_3 (sapphire), although SiC and Si substrates are also used [1]. The significant, $\approx 15\%$, lattice mismatch between GaN and sapphire leads to a high density, 10^8 – 10^{10} cm^{-2} , of threading dislocations through the crystal in the (0001)-direction. Despite this, nitride-based optical devices have excellent properties. Evidently, the high dislocation density in the nitrides has less detrimental effects than in other semiconductor systems.

Clear improvement on device material is observed when the dislocation density is reduced; see e.g. [2–4]. Despite this, relatively little work has been done on quantitative studies. A clear correlation between reduced photoluminescence (PL) intensity and mobility as a function of dislocation density has been shown [5–8]. Further, a few models have been developed to describe the detrimental effect of the dislocations. The reduction in PL intensity from non-radiative electron–hole recombinations in dislocations was calculated and compared to experimental values [9]. In another approach, the mobility was calculated due to scattering of electrons at filled traps along dislocation lines [10]. Further, a detailed numerical description of the free electron concentration and mobility due to charged dislocation lines has been made [11]. Due to the high efficiency of high dislocation nitride materials, further investigation is desired to increase our understanding. In this work, we have expanded the model of Gurusinge et al. [11] to predict PL intensity of GaN and compared the model to experimental results.

2. Experimental procedure

Growth of MBE-materials was carried out in a Varian GEN II Modular MBE system on sapphire

substrates mounted indium free. Active nitrogen was provided by a liquid nitrogen cooled Oxford Applied Research CARS25, RF-plasma source. The nitrogen with a purity of 5.5N was further purified to ppb levels by a commercial filter. The MBE-samples consisted of three 400–600 nm thick GaN layers, named B, C and D, grown on c-plane sapphire. After degreasing, the substrates were mounted and outgassed in the growth chamber. Before growing the GaN layer, the sapphire was exposed to nitrogen plasma for 30 min, where the power of the source was 200 W and the nitrogen flow 0.7 sccm. This nitridation process has been shown to simplify further GaN growth due to the formation of an $\text{AlO}_x\text{N}_{1-x}$ alloy layer at the interface which bridges the gap in lattice constants between sapphire and AlN [12]. The GaN layers were grown with a growth rate of $0.2\ \mu\text{m/h}$ at $700\ ^\circ\text{C}$ substrate temperature. However, on two of the samples, B and C, an additional 5 nm AlN buffer layer is grown, at $700\ ^\circ\text{C}$, before GaN deposition.

A MOCVD System (EMCORE D-75) was employed for the growth of one sample, labelled A. Trimethylgallium (TMGa) and ammonia (NH_3) were used as Ga source and N source, respectively. A thermal cleaning process was carried out at $1080\ ^\circ\text{C}$ for 10 min in a stream of hydrogen ambient before the growth of nitride layers. After deposition of a 30-nm-thick GaN nucleation layer at $530\ ^\circ\text{C}$, the substrate was heated up to $1045\ ^\circ\text{C}$ and a 3- μm -thick GaN layer was grown. The flow rate of TMGa was 89.5 mol/min and the flow rate of NH_3 was 3.6 L/min.

The photoluminescence spectra were recorded at 2 K, using a single monochromator (Jobin-Yvon, model HR460) equipped with a CCD camera and a frequency-doubled Ar-ion laser operating at 244.0 nm as an excitation source. The spectral resolution of the system was 0.4 meV. Carrier concentration was determined by capacitance–voltage- (CV) and Hall effect measurements in a Hewlett Packard 4061A Semiconductor Test System. A non-destructive mercury probe from Materials Development Corporation was used to form the CV Schottky contact. I – V measurements from the samples assured us of the quality of the Schottky contact and reliability of our

measurements. For Hall effect measurements, the samples were cleaved into $3 \times 3 \text{ mm}^2$ pieces and indium contacts were soldered in the corners.

To measure the dislocation density of the samples, we followed the method described by Huang et al. [13]. The GaN surface was etched in hot (70°C) phosphoric acid (H_3PO_4). This etchant only attacks the defect sites on the Ga-polar (0001) GaN surface, and the resulting etch-pit density is comparable to the dislocation density determined by other methods. The etch pit density was calculated from atomic force microscopy (AFM) pictures, recorded in tapping mode in a Digital Instruments Dimension 3000 Scanning Probe Microscope. X-ray diffraction (XRD) measurements were made with a Philips Materials Research Diffractometer, equipped with a Bartels Ge(220) four-crystal monochromator and a slit in front of the detector. Scanning electron microscopy (SEM) pictures were taken using a JEOL JSM-6301F scanning electron microscope.

To describe the PL emission we use a model by Gurusinghe et al. [11], where dislocation lines are treated as negatively charged, due to acceptor-like states along their length. A positive space-charge region, with radius R , will be formed around each dislocation to compensate for the negative charge, where R depends strongly on the bulk carrier concentration. Knowing R and the dislocation density, N_{dis} , we can calculate the fraction of the crystal, F , that is free from depletion regions around the dislocations, $F = 1 - N_{\text{dis}}\pi R^2$. Since significant electron–hole recombination is only possible outside of the depletion region, we assume that the PL intensity is directly proportional to F . This way, we have a simple, yet effective, method to quantitatively predict the PL intensity, once the dislocation density and bulk carrier concentration is known.

3. Results

The samples in this study were used because of their variation in defect density. The dislocation density was estimated from AFM pictures of the etch pit density of the different samples. In Fig. 1 can be seen such AFM images. The large image

shows sample A, and the inset, one of the MBE-grown films, C. The different surface features originate in the growth method. Higher temperatures during MOCVD growth lead to smoother surfaces, whereas MBE has a more island-like growth mode. The etching only affects dislocations and, thus, the features are preserved after etching. Interestingly, by counting surface pit features in SEM images of un-etched MBE-grown GaN, a similar value of the dislocation density is obtained, see inset in Fig. 2. However, the surface of as-grown MOCVD-GaN is smooth and dislocation density cannot be estimated from SEM images. Further, a clear correlation is seen between the dislocation density and the full-width at half-maximum (FWHM) of XRD curves, where the density is proportional to the FWHM^2 of symmetrical (0002) ω -rocking curves. The result of the dislocation density measurements is shown in Fig. 2. As seen, regardless of characterization method, a similar value is determined for each individual film, while it differs greatly from sample to sample.

The PL from each sample was recorded. The shape and intensity of the curves were

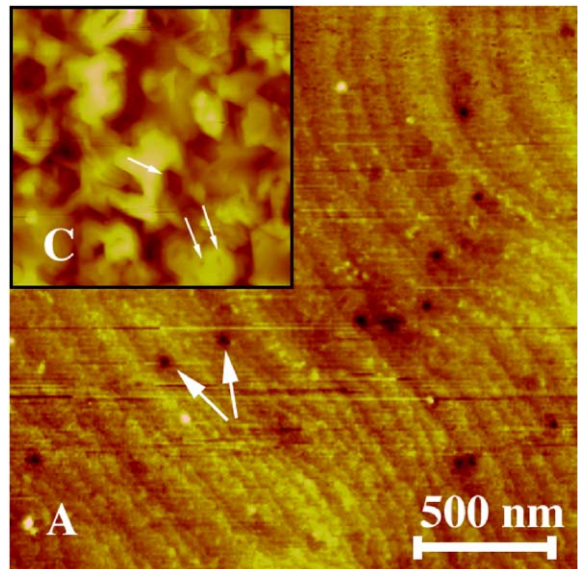


Fig. 1. AFM image of etched GaN surfaces. The arrows point at etch-pits, which are counted to give a value for the dislocation density. Sample A is grown by MOCVD and sample C by MBE.

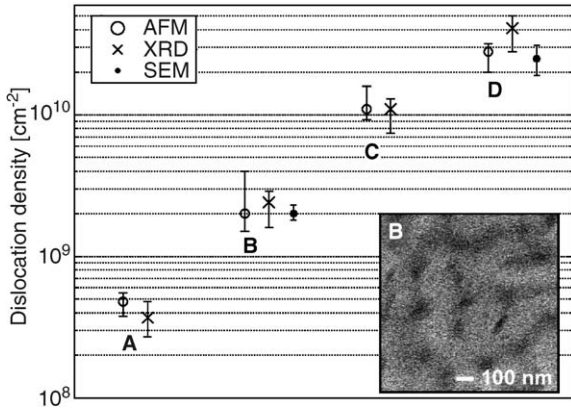


Fig. 2. Summary of dislocation density measurements, including error bars, on samples A–D. AFM measurements were done on etched GaN surfaces and SEM on un-etched. The inset shows a SEM image of sample B, where the pits correspond to dislocations. The XRD results were calculated from FWHM of the GaN (0002) reflection, where the dislocation density is proportional to FWHM².

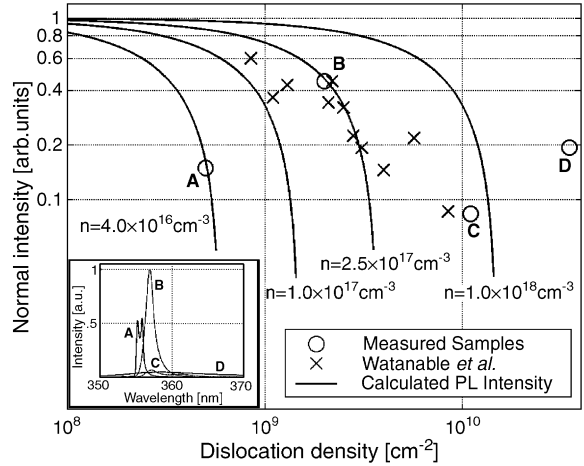


Fig. 3. Calculated and measured PL intensity plotted against dislocation density. The measured carrier concentration of samples A–D were 4×10^{16} , 2.5×10^{17} , 1.0×10^{18} and $2 \times 10^{20} \text{ cm}^{-3}$, respectively. Published samples had a carrier concentration of $1 \times 10^{17} \text{ cm}^{-3}$. The carrier concentration for the calculations is given in the figure. The inset shows the PL curves of samples A–D, measured at 2 K.

reproducible over a large area of each wafer, but differed clearly from film to film. The curves are included in the inset of Fig. 3. To compare the luminescence intensity with the theoretical model, the PL curves were integrated and normalized.

In Fig. 3, the PL intensity is calculated for different carrier concentrations and plotted against dislocation density. We have also included measured data from our samples, as well as published results [8]. The carrier concentrations, used in the calculations, were chosen to be those of the samples in this study. Samples A–C show excellent agreement with calculated results. The previously published data correspond reasonably well with the model. The calculated PL is very sensitive to small changes in the carrier concentration and deviations from the model could be explained by differences between the samples. Also, no information was given of how the intensity was measured, whether it was peak intensities or, as we did it, integrated intensities. Different peak shapes may give different results when integrated over a wide wavelength range. However, the model does not accurately predict the PL intensity from sample D. At these carrier concentrations and dislocation densities, the pre-

dicted intensity is still unity, and the model fails. This sample is grown by MBE without an AlN buffer layer and such GaN films are known to grow with N-polarity [14] as opposed to the favourable Ga-polarity of the other samples in this study. However, the theory makes no distinction between different polarity materials. Although different growth modes of N- and Ga-polarity GaN give rise to material differences [15], it is more likely that we have reached the limit of the model validity. From the calculations it's clear that n-type background doping is favourable for increased PL intensity. Higher carrier concentration means smaller depletion regions and more free carriers. Thus, intentional n-type doping can lead to increased PL efficiency.

4. Conclusion

We have shown that we can quantitatively predict the relative PL intensity from GaN samples using the dislocation density and carrier concentration as parameters. By calculating the depletion

region around the dislocations we get the fraction of the crystal volume where electron–hole recombination is prevented. The assumption that the emitted intensity is inversely proportional to this fraction is shown to be valid for common dislocation densities and carrier concentrations found in typical GaN films. GaN samples of varying crystal quality were thoroughly investigated and compared to the theory.

Acknowledgements

This work was supported financially by SAAB Microtech AB, the Swedish Foundation for Strategic Research and the Swedish National Science Research Council.

References

- [1] S.C. Jain, M. Willander, J. Narayan, R. Van Overstraeten, *J. Appl. Phys.* 87 (2000) 965.
- [2] X.A. Cao, S.F. LeBoeuf, M.P. D'Evelyn, S.D. Arthur, J. Kretchmer, C.H. Yan, Z.H. Yang, *Appl. Phys. Lett.* 84 (2004) 4313.
- [3] P. Gibart, *Rep. Prog. Phys.* 67 (2004) 667.
- [4] T. Miyajima, et al., *J. Phys.: Condens. Matter* 13 (2001) 7099.
- [5] T. Miyajima, et al., *Physica Status Solidi B Fourth International Conference on Nitride Semiconductors, 16–20 July 2001* 228 (2001) 395.
- [6] H.M. Ng, D. Doppalapudi, T.D. Moustakas, N.G. Weimann, L.F. Eastman, *Appl. Phys. Lett.* 73 (1998) 821.
- [7] J.Y. Shi, L.P. Yu, Y.Z. Wang, G.Y. Zhang, H. Zhang, *Appl. Phys. Lett.* 80 (2002) 2293.
- [8] A. Watanabe, H. Takahashi, T. Tanaka, H. Ota, K. Chikuma, H. Amano, T. Kashima, R. Nakamura, I. Akasaki, *Jpn. J. Appl. Phys. Part 2 (Letters)* 38 (1999) 1159.
- [9] S.Y. Karpov, Y.N. Makarov, *Appl. Phys. Lett.* 81 (2002) 4721.
- [10] N.G. Weimann, L.F. Eastman, D. Doppalapudi, H.M. Ng, T.D. Moustakas, *J. Appl. Phys.* 83 (1998) 3656.
- [11] M.N. Gurusinge, T.G. Andersson, *Phys. Rev. B* 67 (2003) 235208.
- [12] F. Widmann, G. Feuillet, B. Daudin, J.L. Rouviere, *J. Appl. Phys.* 85 (1999) 1550.
- [13] D. Huang, M.A. Reshchikov, F. Yun, T. King, A.A. Baski, H. Morkoc, *Appl. Phys. Lett.* 80 (2002) 216.
- [14] X.Q. Shen, T. Ide, S.H. Cho, M. Shimizu, S. Hara, H. Okumura, S. Sonoda, S. Shimizu, *J. Crystal Growth* 218 (2000) 155.
- [15] R.M. Feenstra, C. Huajie, V. Ramachandran, C.D. Lee, A.R. Smith, J.E. Northrup, T. Zywietz, J. Neugebauer, D.W. Greve, *Surf. Rev. Lett.* 7 (2000) 601.